

# Continuous-wave, multiple-order rotational Raman generation in molecular deuterium

J. T. Green, J. J. Weber, and D. D. Yavuz\*

Department of Physics, 1150 University Avenue, University of Wisconsin at Madison, Madison, Wisconsin 53706, USA

\*Corresponding author: yavuz@wisc.edu

Received November 5, 2010; revised January 19, 2011; accepted February 10, 2011;  
posted February 15, 2011 (Doc. ID 137766); published March 9, 2011

We demonstrate the generation of  $\approx 10$  rotational sidebands using continuous-wave stimulated Raman scattering in molecular deuterium. The generation occurs inside a high-finesse cavity at molecular gas pressures of  $\approx 0.1$  atm. © 2011 Optical Society of America

OCIS codes: 140.3550, 290.5910, 190.5650.

Although Raman scattering originally emerged as a powerful spectroscopic tool, it continues to find new and exciting applications. For example, multiple-order stimulated Raman scattering can be used to produce a broad, coherent spectrum covering many octaves of bandwidth [1,2]. Such a broad spectrum can, in turn, be used to synthesize ultrashort optical pulses. Using this approach, the Harris group and others have demonstrated the first optical pulses to break the single-cycle barrier: pulses so short that there is less than one optical cycle under the envelope of the pulse [3,4]. Recently, there have been a number of exciting improvements on this technique, including the generation of a Raman comb with a constant carrier-envelope phase [5] and the synthesis of quasiperiodic optical pulses [6].

In molecular gases, the Raman cross sections are weak, and as a result, the experiments mentioned above required high-peak-power pulsed lasers. For certain applications, such as precision spectroscopy, extension of these experiments to the continuous-wave (CW) domain is desirable [7]. To achieve the required high intensities with CW laser beams, one approach is to place the molecules inside a cavity with a high finesse both at the pump and at the generated wavelengths. By using this technique, Carlsten and colleagues have demonstrated CW Raman laser thresholds as low as 1 mW and conversion efficiencies exceeding 65% [8,9]. Building on this work, Zaitsev *et al.* have demonstrated efficient CW rotational Raman generation at the anti-Stokes wavelength by tuning the cavity resonances with the help of a dispersive gas [10]. We have demonstrated CW light modulation at a frequency of 90 THz using vibrational generation in molecular deuterium ( $D_2$ ) [11]. Despite these exciting developments, ultrashort pulse synthesis using CW-stimulated Raman scattering has not yet been demonstrated. The key obstacle is that the number of generated sidebands has been limited to at most three, which prohibits well-defined pulse synthesis.

In this Letter, we report an experiment that significantly improves on this limitation and that may lead to the synthesis of single-cycle pulses using CW spectral components. Specifically, (1) we demonstrate the generation of up to seven sidebands (two anti-Stokes and five Stokes) with a combined average power exceeding 50 mW using  $|J = 0\rangle \rightarrow |J = 2\rangle$  rotational transition in molecular  $D_2$ . We achieve this generation at a pressure

of 10 Torr (0.013 atm), which is more than 2 orders of magnitude lower than pressures used in typical CW Raman experiments. (2) At pressures of about 80 Torr, we observe simultaneous  $|J = 0\rangle \rightarrow |J = 2\rangle$  and  $|J = 1\rangle \rightarrow |J = 3\rangle$  rotational Raman scattering and demonstrate the generation of more than 10 sidebands. Compared to our previous work [12], the key experimental change that resulted in such high-order generation is the cooling of  $D_2$  molecules to 77 °K with liquid nitrogen ( $N_2$ ).

We proceed with a detailed description of our experiment. Our laser system consists of a custom-built external cavity diode laser at a wavelength of  $1.064 \mu\text{m}$  whose output is amplified with a CW ytterbium fiber amplifier. We couple the amplifier output to the fundamental Gaussian mode of the cavity and use the Pound–Drever–Hall technique to lock to one of the longitudinal modes. Further details regarding our laser and locking systems can be found in our previous publications [11,12]. The cavity consists of two high-reflectivity mirrors inside a custom-made vacuum chamber that we fill with molecular  $D_2$ . The chamber is machined from stainless steel with an inner tube diameter of 5 cm. As shown in Fig. 1, the central 50-cm-long region of the chamber is surrounded by a liquid  $N_2$  reservoir. The chamber has two end-pieces that are removable and are designed to mate with a standard KF flange. These end-pieces house the mirrors of the cavity and

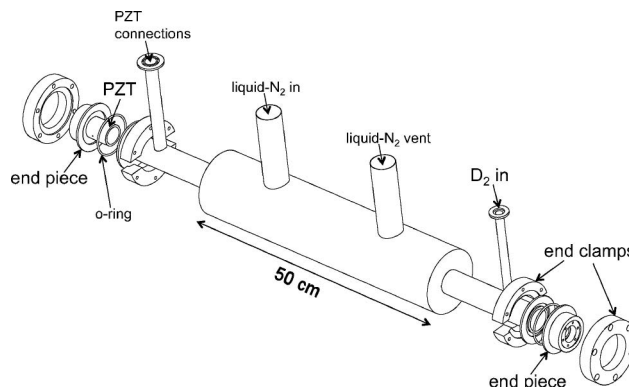


Fig. 1. Stainless steel vacuum chamber that houses the high-finesse cavity (the drawing is to scale). The central 50-cm-long section is surrounded by a liquid  $N_2$  reservoir. The chamber end-pieces hold the cavity mirrors and antireflection coated chamber windows. One of the end-pieces houses the PZT that allows adjustments of the cavity length.

antireflection-coated, vacuum-tight windows. We attach the end-pieces to the main chamber with custom end-clamps and a Viton O-ring. Adjusting the tightness of six screws in each clamp allows for precision control of the pitch of the end-pieces (and therefore the mirrors) within 1 mrad, thereby allowing cavity alignment. We have found these adjustments to be essential, because although the chamber is accurately machined, cooling the system results in undesired structural changes for which precision compensation is necessary.

The mirrors of the cavity have ultralow-loss, high-reflectivity dielectric coatings with a large CW optical damage threshold. The reflectivity is  $\approx 99.99\%$  within a wavelength range of 1.00–1.15  $\mu\text{m}$ . The mirrors have a radius of curvature of 100 cm, and the length of the cavity is 75 cm, giving a free spectral range of 200 MHz. One of the mirrors is mounted on a piezoelectric transducer (PZT) that allows slight adjustments of the cavity length. Cooling  $\text{D}_2$  molecules with liquid  $\text{N}_2$  increases the population of the ground rotational level ( $J = 0$ ) to 54% and decreases the low-pressure Doppler linewidth to 15.5 and 25.8 MHz for the  $|J = 0\rangle \rightarrow |J = 2\rangle$  and  $|J = 1\rangle \rightarrow |J = 3\rangle$  transitions, respectively. The collisional broadening coefficients for the two lines at 77 °K are 0.64 MHz/Torr and 0.42 MHz/Torr, respectively [13].

When we lock the linearly polarized pump laser beam to the cavity, we observe multiple-order rotational stimulated Raman scattering. At low pressures, we find scattering on the  $|J = 0\rangle \rightarrow |J = 2\rangle$  transition at a frequency of  $179\text{ cm}^{-1}$  (5.4 THz) to be dominant. Figure 2 shows a typical spectrum that we observe on an optical spectrum analyzer at a  $\text{D}_2$  pressure of 10 Torr. We observe the generation of up to two anti-Stokes (AS1, AS2) and five Stokes (S1–S5) beams in addition to the pump laser. The spectral components range from 1.03 to 1.18  $\mu\text{m}$  in wavelength. In agreement with the observations of Imasaka and colleagues [14], we predict that the Stokes sidebands are generated through cascade-stimulated Raman scattering, i.e., each Stokes sideband behaves as an independent pump and produces the subsequent Stokes beam through Raman lasing at a cavity mode. The pump and the Stokes beams drive the coherence (off-diagonal density matrix element) of the Raman transition. This generated coherence then mixes with the pump to produce the anti-Stokes beams through four-wave mixing. The anti-Stokes beams are weak, since their frequencies do not coincide

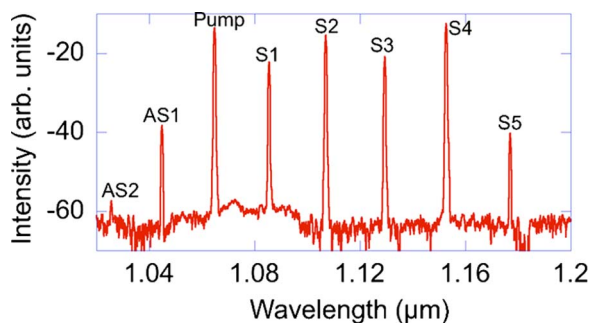


Fig. 2. (Color online) Typical spectrum measured by an optical spectrum analyzer at a  $\text{D}_2$  pressure of 10 Torr (the relative vertical scale is in decibels). We observe multiple-order rotational stimulated Raman scattering on the  $|J = 0\rangle \rightarrow |J = 2\rangle$  transition.

with the cavity resonances [10]. We note that cascade CW-stimulated Raman scattering has also been observed in silicate fibers using multiple fiber Bragg gratings [15]. The key difference of our work compared to fiber-based systems is that since the generation is achieved inside a high-finesse cavity, each of the generated components is predicted to have a linewidth at the kilohertz level. In contrast, solid-state fiber-based systems typically produce output with a bandwidth of a fraction of a nanometer.

Figure 3 shows the sideband powers transmitted through one of the mirrors as a function of the incident pump beam power at a  $\text{D}_2$  pressure of 10 Torr. The maximum sideband powers that we generate are 60  $\mu\text{W}$  (AS1), 17.5 mW (pump), 2.4 mW (S1), 9.2 mW (S2), 2.9 mW (S3), 24.5 mW (S4), and 43  $\mu\text{W}$  (S5). The fifth Stokes sideband (S5) is weak due to a significant drop in the mirror reflectivity at its wavelength. As we increase  $\text{D}_2$  pressure, we observe more evenly distributed sideband powers with reduced total combined power. The reduction in combined power with increasing pressure is likely a result of (1) changes in the cavity mode due to Raman thermal lensing effects as demonstrated by Brasseur *et al.* [16] or due to nonlinear Raman self-focusing or defocusing and (2) reduction in the performance of the cavity lock as a result of large pump depletion and the temporal dynamics of the Raman lasing process.

At higher pressures, we also observe additional generation on the  $|J = 1\rangle \rightarrow |J = 3\rangle$  transition at a frequency of  $297\text{ cm}^{-1}$  (8.9 THz). We find the competition between  $|J = 0\rangle \rightarrow |J = 2\rangle$  and  $|J = 1\rangle \rightarrow |J = 3\rangle$  generation to be sensitive to the mirror alignment, tuning of the cavity length, and absolute frequency of the pump laser beam. The sensitivity is likely a result of the changing frequency overlap between the longitudinal modes of the cavity and the Raman transition line shapes. We have not investigated the competition between the two rotational transitions in detail, and a thorough discussion is left for a future publication. Figure 4 shows a typical generated spectrum at a  $\text{D}_2$  pressure of 80 Torr and an incident pump power of 9 W. Here, the pump beam generates the first Stokes sideband on the  $|J = 1\rangle \rightarrow |J = 3\rangle$  transition, which we denote  $P'$ .

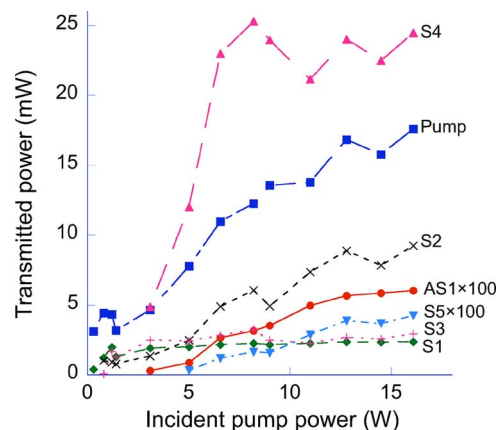


Fig. 3. (Color online) Generated sideband powers as a function of incident pump power at a  $\text{D}_2$  pressure of 10 Torr. The error bars, which are not shown to increase clarity, are about  $\pm 20\%$  at each data point. The largest contribution to the error bars is day-to-day variation due to systematic drifts in the experiment, such as in the alignment of the cavity mirrors.

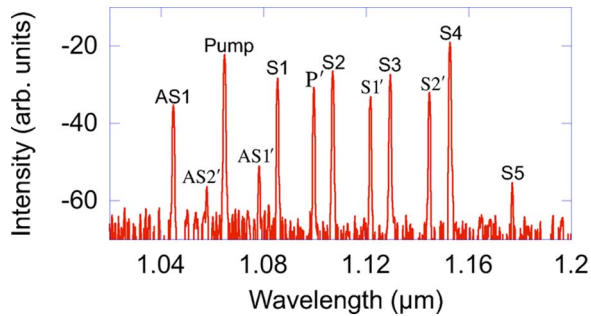


Fig. 4. (Color online) The measured spectrum at a  $D_2$  pressure of 80 Torr and an incident pump of 9 W (the relative vertical scale is in decibels). The beam  $P'$  is the first Stokes on the  $|J = 1\rangle \rightarrow |J = 3\rangle$  transition at a transition frequency of 8.9 THz. This beam then acts as another pump beam and produces another comb of Raman sidebands on the  $|J = 0\rangle \rightarrow |J = 2\rangle$  transition. This new comb is denoted with primed coordinates (AS2' through S2').

This beam then acts as a new pump and generates a new set of sidebands on the  $|J = 0\rangle \rightarrow |J = 2\rangle$  transition. We denote the anti-Stokes and Stokes sidebands generated through this process with primed labels. The total optical power in the generated spectrum of Fig. 4 is approximately 25 mW.

We next discuss the application of our work to temporal waveform synthesis. One drawback of the present approach is that, because the Stokes sidebands are produced through cascade-stimulated Raman scattering, the frequency difference between adjacent spectral components is not constant across the spectrum. Although this is a significant drawback, this variation in frequency differences can, in principle, be measured using nonlinear optical mixing methods. By using frequency tuning elements in the path of each sideband (such as acousto-optic modulators), one can then produce an equidistant Raman comb. For only three beams, the frequency tuning can also be accomplished by tuning the resonance frequencies of the cavity using, for example, the dispersion of a gas [17]. The spectral components can then be thought of as separate, narrow-linewidth, equidistant laser oscillators. The phases of these beams can be actively locked by using beat signals obtained using nonlinear mixing [18]. For the ideal case of phase-locked spectral components with comparable spectral amplitudes, the

spectrum of Fig. 2 would then synthesize approximately 20-fs-long optical pulses with a pulse spacing of 186 fs. In the future, by combining this work with vibrational Raman generation [11], it may be possible to generate a multioctave spectrum with a large number of spectral components.

We thank D. Sikes, N. Proite, and Z. Simmons for experimental assistance and helpful discussions. This work is supported by the National Science Foundation (NSF).

## References

1. A. V. Sokolov, D. R. Walker, D. D. Yavuz, G. Y. Yin, and S. E. Harris, *Phys. Rev. Lett.* **85**, 562 (2000).
2. J. Q. Liang, M. Katsuragawa, F. Le Kien, and K. Hakuta, *Phys. Rev. Lett.* **85**, 2474 (2000).
3. M. Y. Shverdin, D. R. Walker, D. D. Yavuz, G. Y. Yin, and S. E. Harris, *Phys. Rev. Lett.* **94**, 033904 (2005).
4. W. Chen, Z. Hsieh, S. Huang, H. Su, T. Tang, C. Lin, C. Lee, R. Pan, C. Pan, and A. H. Kung, *Phys. Rev. Lett.* **100**, 163906 (2008).
5. T. Suzuki, M. Hirai, and M. Katsuragawa, *Phys. Rev. Lett.* **101**, 243602 (2008).
6. D. D. Yavuz, D. R. Walker, M. Y. Shverdin, G. Y. Yin, and S. E. Harris, *Phys. Rev. Lett.* **91**, 233602 (2003).
7. F. Couny, F. Benabid, and P. S. Light, *Phys. Rev. Lett.* **99**, 143903 (2007).
8. L. S. Meng, P. A. Roos, K. S. Repasky, and J. L. Carlsten, *Opt. Lett.* **26**, 426 (2001).
9. L. S. Meng, P. A. Roos, and J. L. Carlsten, *Opt. Lett.* **27**, 1226 (2002).
10. S. Zaitsev, H. Izaki, and T. Imasaka, *Phys. Rev. Lett.* **100**, 073901 (2008).
11. J. T. Green, J. J. Weber, and D. D. Yavuz, *Phys. Rev. A* **82**, 011805(R) (2010).
12. J. T. Green, D. E. Sikes, and D. D. Yavuz, *Opt. Lett.* **34**, 2563 (2009).
13. H. G. M. Edwards, D. A. Long, and G. Sherwood, *J. Raman Spectrosc.* **22**, 607 (1991).
14. S. Zaitsev, C. Eshima, K. Ihara, and T. Imasaka, *J. Opt. Soc. Am. B* **24**, 1037 (2007).
15. Z. Luo, C. Huang, G. Sun, H. Xu, Y. Wang, C. Ye, and Z. Cai, *Opt. Commun.* **265**, 616 (2006).
16. J. K. Brasseur, R. F. Teehan, P. A. Roos, B. Soucy, D. K. Neumann, and J. L. Carlsten, *Appl. Opt.* **43**, 1162 (2004).
17. S. Zaitsev and T. Imasaka, *Appl. Opt.* **49**, 1586 (2010).
18. T. W. Hansch, *Opt. Commun.* **80**, 71 (1990).